Application of material forces in finite element simulations

Authors:

S. Kolling, D. Ackermann
DaimlerChrysler AG, Sindelfingen, Germany

Correspondence:

Dr. Stefan Kolling
DaimlerChrysler AG
HPC X411
D-71059 Sindelfingen
Germany

Tel: +49-(0)7031 - 9082829
Fax: +49-(0) 7031 - 9078837
e-mail: stefan.kolling@daimlerchrysler.com

Keywords:
Configurational Forces, Explicit Finite Element Method, Hyper-elasticity,
Dynamic Fracture Mechanics, J-Integral

ABSTRACT

Presented is a theoretical description and computational method to calculate configurational forces in the context of the finite element method. We take fully 3D-case, dynamics and large deformations in hyper-elastic materials into account. The FE implementation and numerical analysis of different structures demonstrates the applicability of the constitutive description. In our derivation, the Lagrangian depends on the deformation gradient and on the position (in the reference configuration) explicitly, which accounts for inhomogeneous materials, e.g. materials with phase boundaries, voids or cracks. In analogue to the local balance of momentum, the so-called Eshelby stress holds a configurational force balance (balance of momentum for the material motion problem), where configurational (or material) forces correspond to the volume forces in the physical space. An FE description is obtained by formulating the weak form of the configurational force balance. Thus, the configurational forces acting on the finite element nodes may be computed as the physical boundary value problem is solved. For the static case and small deformations, the configurational force corresponds to the well known J-Integral in fracture mechanics.

1. INTRODUCTION

In many fields of industrial application, the mechanism and prediction of fracture processes play a dominant role. Especially in problems of short-time dynamics, such as crash simulation and military applications, the question of crack-propagation is still an important field of research. The basis for the treatment of cracked structures is the energy release rate during a virtual displacement of the crack-tip: the so-called J-integral introduced by Rice (1968). Although many commercial FE-codes are able to calculate the J-integral, the results are restricted to simple cases like crack mode-I, small deformations and quasi-static loading.

In a more general context, the theory of configurational forces has been established as a useful tool to investigate an energy change of an inhomogeneous continuum mechanical system. Configurational forces allow the numerical simulation in a wide range of mechanics and material science.

The idea of calculating configurational forces with finite elements goes back to the work of Braun (1997). Especially with respect to fracture mechanics, this numerical technique has been applied in the papers by Steinmann (2000), Steinmann, Ackermann and Barth (2001) and Mueller, Kolling and Gross (2002). In Mueller, Kolling and Gross (2002), it is shown how configurational forces can be used to improve discretization meshes and in a later work, Mueller and Maugin (2002), configurational forces are used to simulate mixed mode crack propagation.

In the static case, the change of the energy is given by the gradient of the total potential. The result is a generalised force, which is called the configurational (or material) force and was first introduced by Eshelby (1951). The physical meaning of this force is given by the considered problem: direction of diffusion, dislocation movement or crack propagation among others. In the dynamic case, the change of the energy is given by the gradient of the Lagrangian, i.e. the difference of kinetic and strain energy. This results in the so-called dynamic energy momentum tensor which, likewise, was introduced by Eshelby. In the present paper, we recast Eshelby's ideas to derive a generalised (configurational) balance equation. A weak formulation of this balance equation is used to obtain the configurational forces by finite elements very efficiently.

In this first application, we restrict our attention to hyper-elastic materials. However, the extension of the theory towards plasticity and visco-elasticity is possible and has

been carried out, e.g. see the books by Maugin (1993), Gurtin (2000) and Kienzler and Herrmann (2000).
As some illustrative examples, we investigate the configurational forces at the boundary of a two-phase bar during dynamic loading, a compact tension test and an impact test using LS-DYNA.

2. BASIC EQUATIONS: THE PHYSICAL SPACE

We consider a homogeneous body B , density ρ_0, with body forces f_i. In our derivations, Cartesian coordinates and the index notation are used for more clarity. The small indices (e.g. x_i) denote coordinates with respect to the actual (material) configuration and the capitals (e.g. X_J) stand for the reference configuration. In a hyperelastic continuum, there exists a strain energy function $W = \hat{W}(F_{iJ})$ from which the stresses can be obtained by derivation:

$$P_{iJ} = \frac{\partial W}{\partial F_{iJ}} . \tag{1}$$

Here, $F_{iJ} = \partial x_i / \partial X_J$ is the deformation gradient and P_{iJ} is the first Piola-Kirchhoff stress-tensor. With the stress-tensor in (1), the local form of the momentum balance can be written as

$$P_{iJ,J} + f_i = \rho_0 \dot{v}_i , \tag{2}$$

where v_i is the (local) velocity.
The second Piola-Kirchhoff (pseudo) stress $S_{IJ} = 2\partial W / \partial C_{IJ}$ is obtained by deriving the energy function with respect to the right Cauchy-Green strain tensor $C_{IJ} = F_{kI} F_{kJ}$. First and second Piola-Kirchhoff stresses are related by $P_{Kj} = S_{KL} F_{jL}$. The (true) Cauchy stress σ_{ij} can be obtained by forming

$$\sigma_{ij} = J^{-1} F_{iK} P_{Kj} = J^{-1} F_{iK} S_{KL} F_{jL} , \tag{3}$$

where $J = \det F_{iJ}$ is the relative volume.

3. CONFIGURATIONAL FORCES: THE MATERIAL SPACE

Now, we generalise our continuum and consider the body B to be inhomogeneous. For such a body, we derive a balance equation which has the same structure as the momentum balance (2) for the homogeneous body. The Lagrangian $L = T - W$ of the system is defined as the difference of the kinetic energy

$$T = \hat{T}(\rho_0, v_i) = \frac{1}{2}\rho_0 v_i v_i \tag{4}$$

and the strain energy $W = \hat{W}(F_{iJ}, X_K)$. Now, the strain energy depends on the deformation gradient F_{iJ} and on the position X_K explicitly to consider inhomogeneous materials. Formulating the gradient of the Lagrangian yields

$$\frac{\partial L}{\partial X_K} = \frac{\partial T}{\partial X_K} - \frac{\partial W}{\partial X_K} = \frac{\partial T}{\partial \rho_0}\frac{\partial \rho_0}{\partial X_K} + \frac{\partial T}{\partial v_i}\frac{\partial v_i}{\partial X_k} - \frac{\partial W}{\partial F_{iJ}}\frac{\partial F_{iJ}}{\partial X_K} - \left.\frac{\partial W}{\partial X_K}\right|_{\text{expl}}. \tag{5}$$

Using (1) and (4), we obtain

$$\frac{\partial T}{\partial \rho_0} = \frac{1}{2}v_i v_i, \quad \frac{\partial T}{\partial v_i} = \rho_0 v_i \quad \text{and} \quad \frac{\partial W}{\partial F_{iJ}} = P_{iJ} \tag{6}$$

and (5) can be rewritten:

$$L_{,K} = \frac{1}{2}v_i v_i \rho_{0,K} + \rho_0 v_i v_{i,K} - P_{iJ}F_{iJ,K} - \left.\frac{\partial W}{\partial X_K}\right|_{\text{expl}} \tag{7}$$

Inserting $v_{i,K} = \dot{F}_{i,K}$, $F_{iJ,K} = F_{iK,J}$, the identity $P_{iJ}F_{iK,J} = \left(P_{iJ}F_{iK}\right)_{,J} - P_{iJ,J}F_{iK}$ and (2) yields

$$L_{,K} = \frac{1}{2}v_i v_i \rho_{0,K} + \rho_0 v_i \dot{F}_{iK} - \left(P_{iJ}F_{iK}\right)_{,J} + \underbrace{P_{iJ,J}}_{=\rho_0 \dot{v}_i - f_i} F_{iK} - \left.\frac{\partial W}{\partial X_K}\right|_{\text{expl}}$$

$$\Leftrightarrow$$

$$-L_{,J}\delta_{KJ} - \left(P_{iJ}F_{iK}\right)_{,J} + \frac{1}{2}v_i v_i \rho_{0,K} - f_i F_{iK} - \left.\frac{\partial W}{\partial X_K}\right|_{\text{expl}} = -\rho_0 v_i F_{iK} - \rho_0 v_i \dot{F}_{iK}$$

$$\Leftrightarrow$$

$$\underbrace{\left(-L\delta_{KJ} - P_{iJ}F_{iK}\right)}_{\Sigma_{KJ}}{}_{,J} + \underbrace{\frac{1}{2}v_i v_i \rho_{0,K} - f_i F_{iK} - \left.\frac{\partial W}{\partial X_K}\right|_{\text{expl}}}_{g_K} = -\rho_0 \left(v_i F_{iK}\right)^{\cdot}$$

The second order tensor Σ_{KJ} in the brackets of the left side is called “energy momentum tensor” and the force g_K is the material force (configurational force), see Eshelby (1970). Now, we have a compact equation

$$\Sigma_{KJ,J} + g_K = -\rho_0 \left(F_{iK} v_i\right)^{\cdot}, \tag{8}$$

which has the same structure as the momentum balance (2) and is called “configurational force balance”. A further notation which also can be found in literature is “balance of pseudo-momentum”. From the definition of g_K , configurational forces occur, if:

1. The material is inhomogeneous: $W = \hat{W}(F_{iJ}, X_K)$
2. The density depends on the position $\rho_0 = \hat{\rho}_0(X_K)$
3. Volume forces exist: $f_i \neq 0$

In the static case, the terms in equation (8) are simplified to $\Sigma_{KJ,J} + g_K = 0$, where $\Sigma_{KJ} = W\,\delta_{KJ} - P_{iJ}F_{iK}$ and $g_K = -f_i F_{iK} - \left.\frac{\partial W}{\partial X_K}\right|_{\text{expl}}$.

And for small deformations, the energy momentum tensor is $\Sigma_{kj} = W\,\delta_{kj} - u_{i,k}\sigma_{ij}$. In this case, the 1-component (using $dx_1 = n_1 d\Gamma$) of the material force acting on a crack-tip is related to the J-integral in fracture mechanics, see Rice (1968):

$$J = -\frac{\partial W}{\partial a} = \int_{\Gamma} W\,dx_1 - u_{i,1}\sigma_{ij}n_j\,d\Gamma\,, \tag{9}$$

where Γ is a path surrounding the crack-tip. The interpretation of the J-integral is the energy release rate of the system with respect to a virtual movement δa of the crack-tip along the ligament. The usual way to calculate *J* is to define a path Γ and solve equation (9). The problems we are facing then, is that *J* is not always path independent, e.g. if we have mixed mode loading. In what follows, we show an alternative way to determine *J* consistent with the FE method.

4. FINITE ELEMENTS

4.1 Explicit Finite Element Method

In our simulations, we use the explicit solver of LS-DYNA. In this finite element code, Newton’s equation of motion

$$M_{ij}\,\ddot{x}_j(t) + C_{ij}\,\dot{x}_j(t) + K_{ij}\,x_j(t) = p_i(t) \tag{10}$$

is solved via a central difference method. The matrices M_{ij} , C_{ij} and K_{ij} stand for mass, damping and stiffness of the system, $p_i(t)$ is the external loading. For each time step we have:

$$\dot{x}^n = \frac{1}{2\Delta t}\left(x^{n+1} - x^{n-1}\right) \tag{11}$$

$$\begin{aligned}\ddot{x}^n &= \frac{1}{\Delta t}\left(\dot{x}^{n+\frac{1}{2}} - \dot{x}^{n-\frac{1}{2}}\right) = \frac{1}{\Delta t}\left(\frac{x^{n+1} - x^n}{\Delta t} - \frac{x^n - x^{n-1}}{\Delta t}\right) \\ &= \frac{1}{(\Delta t)^2}\left(x^{n+1} - 2x^n + x^{n-1}\right)\end{aligned} \tag{12}$$

Inserting (12) and (11) in (10) at time t_n yields

$$\begin{aligned}&M_{ij}\left(x_j^{n+1} - 2x_j^n + x_j^{n-1}\right) + \frac{\Delta t}{2} C_{ij}\left(x_j^{n+1} - x_j^{n-1}\right) + (\Delta t)^2 K_{ij} x_j^n \\ &= (\Delta t)^2 p_j^n .\end{aligned} \tag{13}$$

This can be rewritten with respect to the displacement x^{n+1}:

$$\begin{aligned}&\overbrace{\left(\frac{1}{(\Delta t)^2} M_{ij} + \frac{1}{2\Delta t} C_{ij}\right)}^{\hat{M}_{ij}} x_j^{n+1} \\ &= \underbrace{p_j^n - \left(K_{ij} - \frac{2}{\Delta t^2} M_{ij}\right) x_j^n - \left(\frac{1}{(\Delta t)^2} M_{ij} - \frac{1}{2\Delta t} C_{ij}\right) x_j^{n-1}}_{\hat{p}_j^n}\end{aligned} \tag{14}$$

and solved after inverting $\hat{M}_{ij}$:

$$x_i^{n+1} = \hat{M}_{ij}^{-1}\ \hat{p}_j^n \tag{15}$$

4.2 Material Forces

Starting point of the finite element discretization is the weak formulation of the configurational force balance (8). To obtain the weak form, we multiply (8) by a test function η_K and integrate over B:

$$\begin{aligned}&\int_B \left(\rho_0 \left(F_{iK} v_i\right)^{\cdot} + \Sigma_{KJ,J} + g_K\right) \eta_K \, dV = \\ &\int_B \underbrace{(\rho_0 F_{iK} v_i)^{\cdot}}_{=:-P_K} \eta_K + (\Sigma_{KJ}\eta_K)_{,J} - \Sigma_{KJ}\eta_{K,J} + g_K \eta_K \, dV = 0.\end{aligned} \tag{16}$$

Here, is called the pseudo momentum vector. Integrating by parts yields

$$\int_B -\dot{P}_K \eta_K - \Sigma_{KJ} \eta_{K,J} + g_K \eta_K \, dV + \int_{\partial B} \Sigma_{KJ} N_J \eta_K \, dA = 0 . \tag{17}$$

If we consider stationary boundaries, i.e. boundaries which remain fixed, the boundary integral in (17) vanishes. Now, the test function is approximated in every element

$$\eta_K = \sum_l N^l \eta_K^l , \; \eta_{K,J} = \sum_l N^l_{,J} \eta_K^l \tag{18}$$

Inserting (18) in (17) yields:

$$\sum_l \eta_K^l \int_B \left\{ -\dot{P}_K N^l - \Sigma_{KJ} N^l_{,J} + g_K N^l \right\} dV = 0 \tag{19}$$

Since this equation has to be fulfilled for arbitrary η_K^l , the bracket has to be zero and the discrete material forces are given by

$$G_K^l = \int_B g_K N^l \, dV = \int_B \dot{P}_K N^l + \Sigma_{KJ} N^l_{,J} \, dV \tag{20}$$

To obtain the total material force G_K^I acting an the node I, the forces G_K^l of all elements adjacent to node I have to be assembled:

$$G_K^I = \bigcup_{l=1}^{n_e} G_K^l \tag{21}$$

With this formulation, the material forces can be calculated simply as the physical boundary value is solved: all quantities to compute Σ_{KJ} and $\dot{P}_K$ are already known in every time step.

4.3 Implementation into LS-DYNA: algorithm

The material forces have been implemented by the authors as a user-subroutine in the explicit solver LS-DYNA. The basis is a hyper-elastic material as defined by the laws of Blatz and Ko (MT 7), Mooney and Rivlin (MT 27) and Ogden (MT 77). In such a material subroutine, all necessary quantities (F_{iJ} , $\dot{F}_{iJ}$, v_i , $\dot{v}_i$, P_{iJ}) are computed locally in every time-step. From this,

1. calculate the energy momentum tensor $\Sigma_{KJ} = (W\text{-}T)\,\delta_{KJ} - P_{iJ} F_{iK}$
2. calculate the pseudo momentum vector $\dot{P}_K = -\rho_0 \left(\dot{F}_{iK} v_i + F_{iK} \dot{v}_i \right)$
3. solve $G_K^l = \int_B \dot{P}_K N^l + \Sigma_{KJ} N^l_{,J} \, dV$, e.g. via Gauss-quadrature.
4. assemble all material forces according to (21).

5. APPLICATIONS

For the first application in LS-DYNA, we calculate the material forces in the situation of a two-phase bar, a compact tension test and an impact test. The calculations are executed under plane stress condition using Belytschko-Tsai shell elements with one integration point both in the shell plane and in the shell thickness. All values are relative to a unit thickness because of the 2D-case.

5.1 Two-Phase Bar

As a first example, we investigate a simple bar under tension. The bar consists of two materials which are separated by an interface. The system is sketched in Figure 1. We chose a stiffness of E_1=*210*GPa, $E_2=E_1/2$=*105*GPa, $l/2=h$=*10*mm. In the FE calculation, the Poisson ratio is zero to catch the 1D case. The load *u(t)* is increased linearly from *0.0*mm to *0.1*mm in *t0=0.1*ms. The loading process may assumed to be quasi-static. For this case, an analytical (static) solution exists:

$$G = 2\frac{u^2(t)E_1E_2A[E_2 - E_1]}{l^2[E_1 + E_2]^2} = 11.67N$$

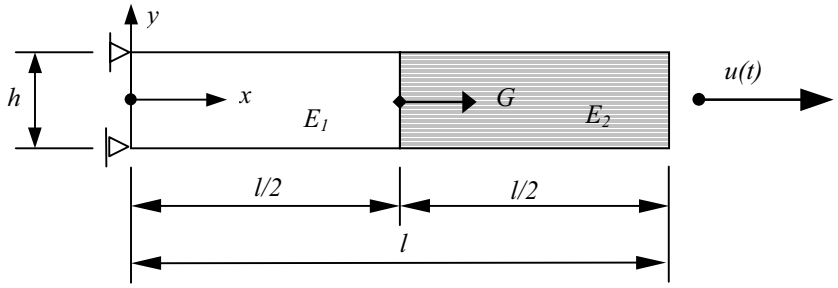

Figure 1 two-phase bar

The results of the 2D finite element calculation are shown in Figure 2. As emphasized in the theoretical part, material forces always appear at the boundary of the system and, due to the inhomogeneity, at the phase boundary.

a) two elements b) eight elements

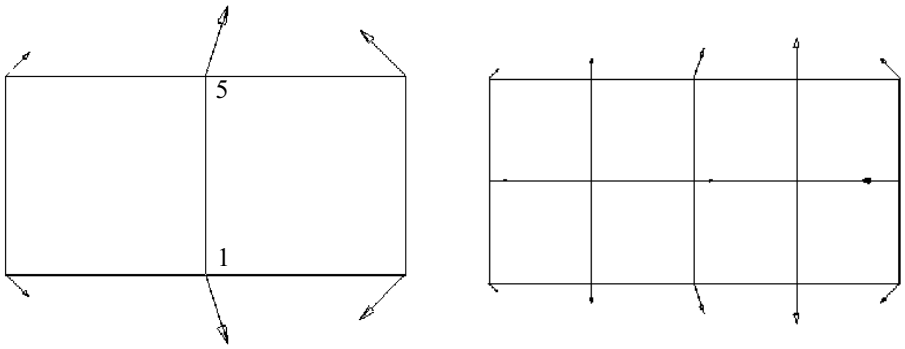

Figure 2 2d-bar, 4-node-elements, material forces

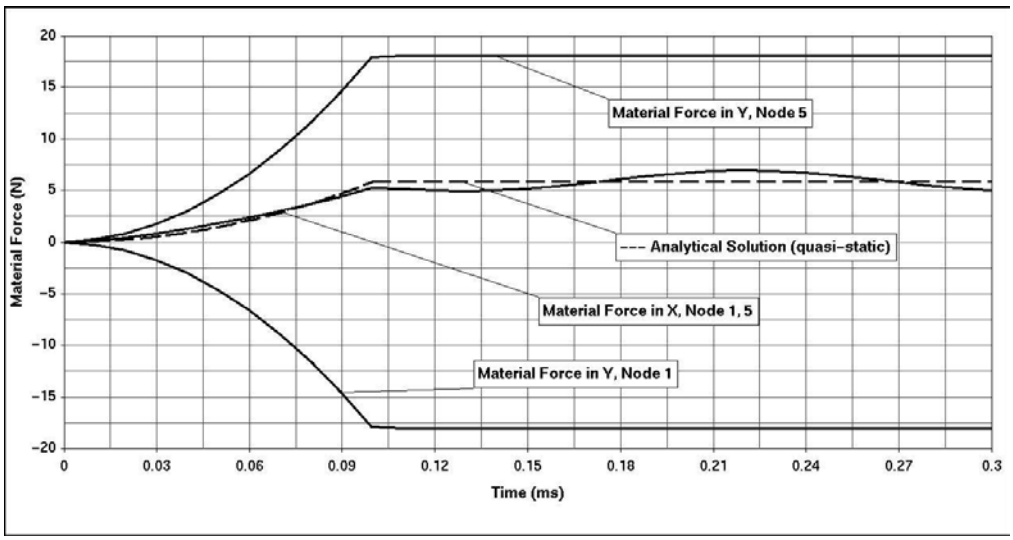

Figure 3 2d-bar, validity test, quasi-static

The physical meaning of the material forces is the direction of a possible diffusion process: The phase boundary tries to migrate to the harder material to achieve an energetic minimum. Figure 3 shows the temporal evolution of the forces in time. The material force in *x*-direction increases monotonously till *t0=0.1*ms and oscillates, then, around the analytical solution (dashed line). The average value of this oscillation gives the analytical solution (*G=11.67/2=5.833*N for each node in Figure $2_{a)}$). The material force in *y*-direction is positive at node 5 and negative at node 1. The resultant in *y* is zero for the 1D-bar.

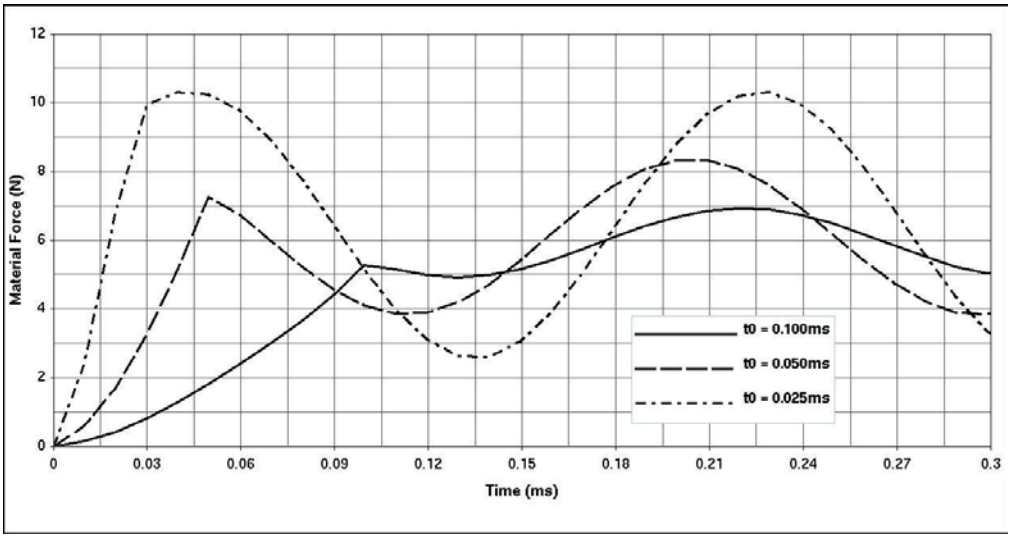

Figure 4 2d-bar, different loading rates

In Figure 4, we vary the loading rate from *0.1*ms, *0.025*ms to *0.05*ms. Because of the higher kinetic energy part, a significant increase of the amplitude and the average

value of the material force can be detected for higher loading rates. This behaviour is important to know for the interpretation of material forces in short-time dynamics applications.

5.2 Compact Tension (CT) Test

As a further example, we calculate the material forces acting on the crack-tip of a CT specimen (*E=210*GPa). In Figure 5, the specimen is loaded at the nodes of the upper bore hole by a displacement *u(t)* in *y*. The load is increased linearly from *0.0*mm to *1.0*mm in *t0=0.1*ms. Again, the loading process may assumed to be quasi-static.
At the lower one the nodes are translationally fixed. This results in a bending which leads to a non-symmetric case. Thus, we have a mixed-mode loading and the material force has both a component in *x* and in *y*-direction. A possible crack propagation takes place in a certain angle to the *x*-axis (reverse to the direction of *G*). It should be mentioned that, because of the singularity, the mesh surrounding the crack-tip has to be very fine for an exact calculation of the magnitude of the J-integral. Thus, the calculated material force is not exactly *J*. However, the direction is given and it converges to *J* for a fine mesh, see Mueller, Kolling and Gross (2002) for such a study. In Steinmann, Ackermann and Barth (2001), eight-node elements are used for a SET-specimen: If interior nodes at the crack-tip are moved to the quarter position, the exact value of the *J*-Integral can be obtained.
If we take the same boundary condition at both bore holes, the stress field is symmetric and the material force has solely a component in *x*-direction. Now, a possible crack propagation takes place in the ligament. This situation is depicted in Figure 6.
In the Figures, the displacements are scaled by the factor *2.0* for a better visualisation.

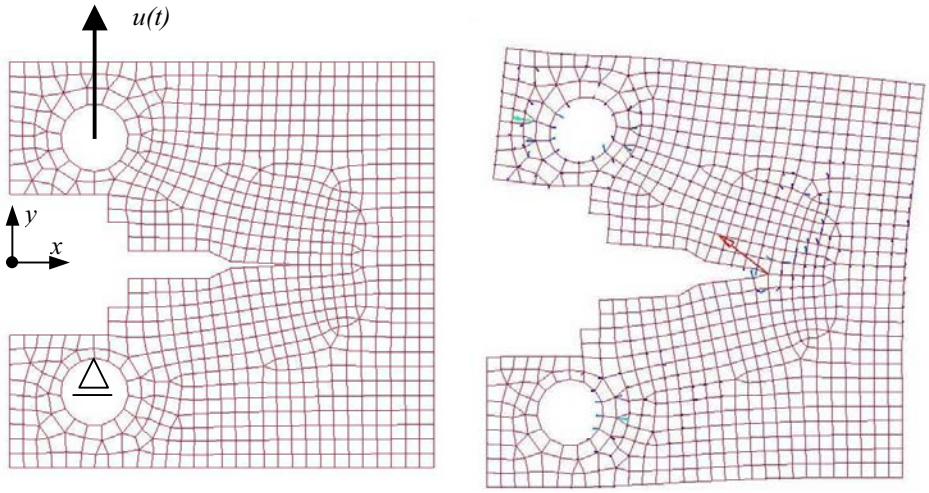

Figure 5 Material forces on a CT specimen, non-symmetric case

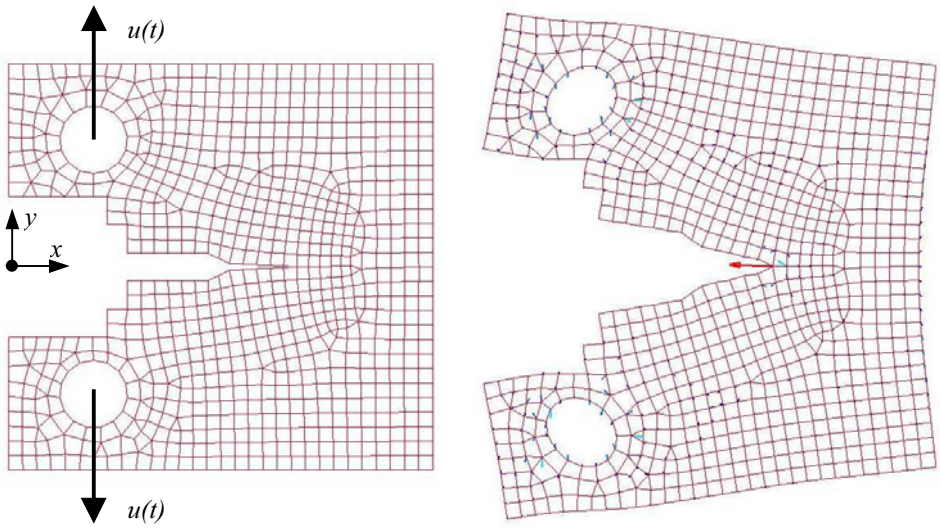

Figure 6 Material forces on a CT specimen, symmetric case

5.3 Impact Test

As a last example, we consider a cylindrical impactor (*d=10*mm, *m=6*kg, *v=10*m/s, rigid) impacting on beam (*l=100*mm, *h=20*mm, Steel) with a centrally located crack (*a=5*mm). The beam is bearing supported in *y*-direction as given in Figure 7. For the contact condition, we use the formulation “AUTOMATIC_SINGLE_SURFACE”.

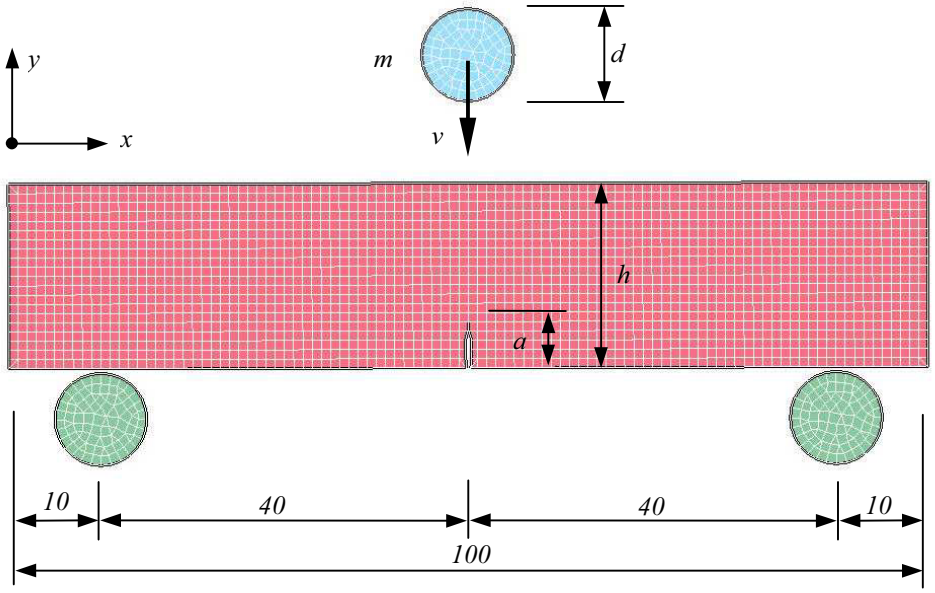

Figure 7 Impact test

The material forces, which occur during this impact are shown in Figure 8 for the maximum loading at *t=0.24*ms. Large configurational forces exist in the contact zone of the impactor, the bearing and, of course, near the crack-tip. In each of this region, the mesh has to be refined to increase the degree of precision. In the other regions, the mesh may even be coarsened. The application of material forces in an adaptive strategy is outlined in detail by Mueller and Maugin (2002). The material force at the crack tip shows again the negative direction of a possible crack propagation. Due to the (almost) symmetric load case, we have a mode-I crack and the material force has only a component in y-direction.

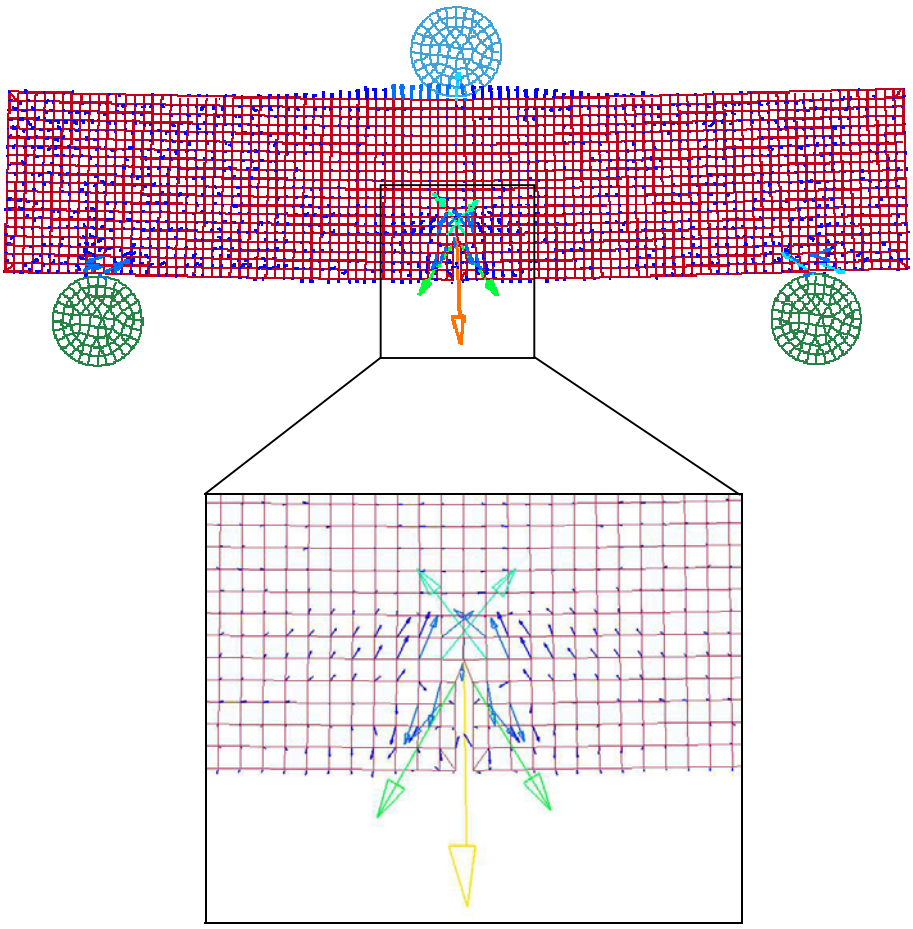

Figure 8 Material forces during an impact test, t=0.24ms

Finally, the temporal evolution of the Material forces at the crack tip is shown in Figure 9. During the calculation, we plotted the material forces every *0.2*ms (dotted line). For a better impression, a SAE filter is used (solid line). The first contact of the impactor takes place at *t=0.06*ms. Then the force increases monotonously towards the

maximum, which is reached at *t=0.24*ms. After *t=0.5*ms the impact process is terminated and the material force vanishes. The run of the curve is proportional to the loading of the beam due to the impact-momentum.

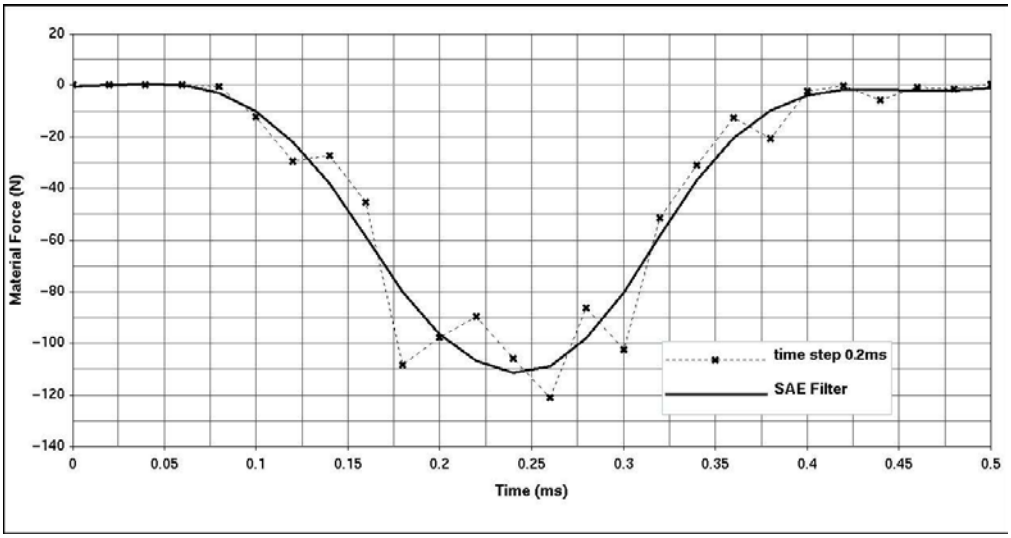

Figure 9 Temporal evolution of the Material forces at the crack tip

6. SUMMARY AND CONCLUSIONS

The theory of configurational forces and a finite element formulation in the context of large deformation and hyper-elasticity has been presented. Here, the discrete configurational forces acting on finite element nodes are obtained consistent with the FE-formulation. The implementation of configurational forces into the explicit finite element code of LS-DYNA as a user subroutine has been shown. Using a two-phase bar for which an analytical solution exists, we have shown the accuracy of the method by using explicit integration. In the aid of a compact tension test, we presented the first step to simulate a J-integral based dynamic crack propagation with LS-DYNA. Further applications have been implied with respect to mesh assessments and adaptive strategies.

Acknowledgement:
The authors acknowledge sincerely Paul A. Du Bois (consulting engineer, Offenbach, Germany), Dr. Klaus Weimar and Kurt Schweizerhof (Dynamore GmbH, Stuttgart, Germany) for helpful discussions on the implementation of a LS-DYNA user subroutine and for the visualisation of the configurational forces in LS-POST.

REFERENCES

Braun M. (1997) Configurational forces induced by finite-element discretization. Proc. Estonian Acad. Sci. Phys. Math., **46**(1/2): 24-31.

Eshelby J.D. (1951) The force on an elastic singularity. Phil. Trans. Roy. Soc. A (244): 87-112.

Eshelby J.D. (1970) Energy relations and the energy-momentum tensor in continuum mechanics. In Kanninen M.F. (editor) Inelastic behaviour of solids. McGraw Hill. New York.

Gross D., Mueller R., Kolling S. (2002) Configurational forces - Morphology evolution and finite elements. Mechanics Research Communications, **29**(6): 529-536.

Gurtin M.E. (2000) Configurational forces as a basic concept of continuum physics. Springer Verlag.

Heintz P., Larsson F., Hansbo P., Runesson K. (2002) Adaptive strategies and error control for computing material forces in fracture mechanics. Chalmers finite element center, Preprint 2002-18.

Kienzler R., Herrmann G. (2000) Mechanics in material space. Springer Verlag.

Kolling S., Mueller R., Gross D. (2003) A computational concept for the kinetics of defects in anisotropic materials. Computational Material Science, **26**C: 87-94.

Kolling S., Gross D. (2001) Configurational forces on material defects. Proceedings in Applied Mathematics and Mechanics PAMM, **1**: 163-164.

Maugin (1993) Material Inhomogeneities in Elasticity. Chapman & Hall.

Mueller R., Kolling S., Gross D. (2002) On configurational forces in the context of the finite element method. International Journal of Numerical Methods in Engineering, **53**: 1557-1574.

Mueller R., Maugin P.A. (2002) On material forces and finite element discretizations. Computational Mechanics **29**: 52-60.

Rice J.R. (1968) A path independent integral and the approximate analysis of strain concentration by notches and cracks. J. Appl. Mech., **35**: 379-386.

Rivlin R.S. (1948): Large elastic deformations of isotropic materials. Proc. Roy. Soc. London, 241: 379-397.

Steinmann P. (2000) Application of material forces to hyperelastostatic fracture mechanics I: Continuum mechanical setting. Int. J. Solids Structures, **37**: 7371--7391.

Steinmann P., Ackermann D., Barth F.J. (2001) Application of material forces to hyperelastostatic fracture mechanics II: computational setting. Int. J. Solids Structures, **38**: 5509--5526.

Steinmann P. (to appear) On spatial and material settings of hyperelastodynamics. Acta Mechanica.